



Reconfigurable intelligent surface design in phase-space

Neekar M Mohammed⁽¹⁾⁽³⁾, Stephen C Creagh⁽¹⁾, Sergio Terranova⁽¹⁾, Hamidreza Taghvaei⁽²⁾, Mir Lodro⁽²⁾, Gregor Tanner⁽¹⁾ and Gabriele Gradoni⁽¹⁾⁽²⁾

(1) School of Mathematical Sciences, University of Nottingham, Nottingham NG7 2RD, United Kingdom (e-mail: neekar.mohammed2@nottingham.ac.uk)

(2) George Green Institute for Electromagnetics Research, Department of Electrical and Electronics Engineering, University of Nottingham, Nottingham NG7 2RD, United Kingdom

(3) Department of Mathematics, College of Science, University of Sulaimani, Sulaymaniyah, Kurdistan Region, Iraq

Abstract

Reconfigurable intelligent surfaces are planar structures that dynamically change their reflection or refraction behaviour to engineer complex propagation environments. A physics-based modelling framework is formulated that accounts for the scattered electromagnetic field by an array of reconfigurable unit cells. The model is grounded on finite-size electric/magnetic surface current densities, and develops a wave-dynamical phase space, or angular-positional, representation of scattered waves. The phase-space representation facilitates the integration of intelligent surfaces within Eulerian ray-tracing methods, such as the Dynamical Energy Analysis. The framework is used for evaluating and optimising the design of beam-splitters and anomalous reflectors. A Wigner transform approach is used to devise the field-based phase-space representation. Obtained results are the first step towards the development of a flexible and efficient coverage planning tool for multi-RIS mobile networks.

1 Introduction

Reconfigurable intelligent surface (RIS) technology has recently emerged as a potential candidate for beyond 5G/6G wireless network architectures due to its ability to modulate the wireless propagation environment [1]. A RIS is a thin structure with sub-wavelength features that allow for the dynamic control of the electromagnetic wavefront upon reflection, transmission, and refraction. RISs are used in wireless communications to create so-called programmable and reconfigurable wireless propagation environments, which are wireless environments that are not viewed and treated as random uncontrollable entities but instead become part of the network design that can be optimised through wireless coverage planning [2, 3]. Motivated by these considerations, several authors have investigated scattering from finite-size RISs using various analytical methods and modelling assumptions. In [1, 4, 5, 6, 7, 8], and references therein, a summary of the available contributions, as well as a brief description of their main features and limitations, is presented and discussed. The studies

that are currently available to quantify the potential benefits of embedded RISs in wireless networks are limited to simple network topologies and/or modelling assumptions. State-of-the-art ray models can already efficiently integrate specular reflection and diffraction [1]. However, the electromagnetic (EM) re-radiation from RISs has only recently attracted attention in a ray-tracing context. In particular, Ref. [1] discusses the integration of multi-mode scattering models within ray tracing methods.

In this paper, the angular-spatial re-radiation properties of engineered metasurfaces are modelled through a phase-space approach inspired from the Dynamical Energy Analysis (DEA) [9]. More precisely, we approach the EM radiation problem using the Wigner function (WF) representation of waves. The WF method, which has its origin in quantum mechanics [10], has been intensively studied in the electromagnetic context [11, 12]. Furthermore, the WF has more recently found widespread attention in radio frequency (RF) radiation [11], optics [13] and vibro-acoustic [14, 15]. The main objective of this study is the integration of the RIS response within ray tracing (RT) algorithms in order to achieve a flexible and efficient coverage planning tool for multi-RIS mobile networks upon optimization of the RIS degrees of freedoms.

2 RIS scattered field approximation

Estimating the EM RIS response is based here on the development of a high frequency asymptotic approximation of the RIS scattered field upon oblique incidence of plane waves. We start by considering a transmitter and receiver that are in the far-field of the RIS and do not have direct LOS with each other. The transmitter radiates a uniform TE plane wave that impinges onto a pixelated reflective surface [8]

$$\begin{cases} \mathbf{E}^i = (\hat{\mathbf{y}} \cos \theta^i + \hat{\mathbf{z}} \sin \theta^i) e^{-jk(y \sin \theta^i - z \cos \theta^i)} \\ \mathbf{H}^i = \hat{\mathbf{x}} \frac{1}{\eta} e^{-jk(y \sin \theta^i - z \cos \theta^i)} \end{cases} \quad (1)$$

where η is the free-space wave impedance, k is the wavenumber, and θ^i the incidence angle as shown in Fig.

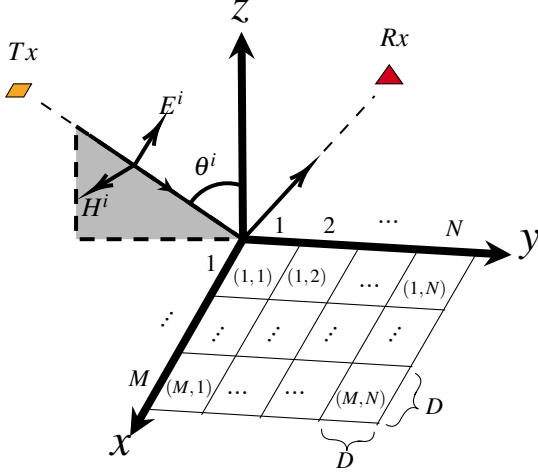


Figure 1. TE-polarized plane wave incident on the RIS [8]. The size of a surface element is $D \times D$, and the total number of elements is $M \times N$, with T_x representing the transmitter and R_x representing the receiver.

1. The plane wave induces an equivalent surface current density on the metasurface of the form

$$\mathbf{J}^s = \hat{\mathbf{y}} \frac{2}{\eta} R_r(m, n) e^{-jk_y \sin \theta^i}, \quad (2)$$

where $R_r(m, n)$ is the reflection coefficient. If each pixel has a unit magnitude reflection coefficient, we introduce the local reflection phase $\psi(m, n)$ using

$$R_r(m, n) = e^{j\psi(m, n)}, \quad (3)$$

with $\psi(m, n) \in \{0, \pi\}$ in a binary RIS. The calculation of the vector potential yields the RIS scattered field

$$\mathbf{E}(\mathbf{p}; r) = \hat{\mathbf{y}} \mathcal{C}(r) \mathcal{E}_y(\theta, \varphi, \theta^i) \mathcal{A}(\theta, \varphi, \theta^i) \quad (4)$$

in the far field, where $\mathcal{C}(r) = -j \frac{kD^2}{2\pi} \frac{e^{-jkr}}{r}$, and the element radiation pattern is defined as

$$\mathcal{E}_y(\theta, \varphi, \theta^i) = \text{sinc } X \text{ sinc } Y \quad (5)$$

and where the RIS array factor is defined as

$$\mathcal{A}(\theta, \varphi, \theta^i) = \sum_{m=1}^M \sum_{n=1}^N e^{j\psi(m, n)} e^{jk p_x m D} e^{jk(p_y - \sin \theta^i) n D}$$

with

$$\begin{aligned} p_x &= \sin \theta \cos \varphi \\ p_y &= \sin \theta \sin \varphi \\ X &= \frac{kD}{2} \sin \theta \cos \varphi \\ Y &= \frac{kD}{2} (\sin \theta \sin \varphi - \sin \theta^i). \end{aligned}$$

Figure 2 illustrates the relationship between the spherical coordinates for the RIS scattered field in the far-field and the momentum variables. The field (4) was used in [8] to optimize the radar cross section (RCS) of binary and quaternary RISs using the Ising model and quantum annealing. Here, we demonstrate how a phase-space simulation approach, such as DEA, can be used to quantify the EM radiation from RIS-assisted propagation environments.

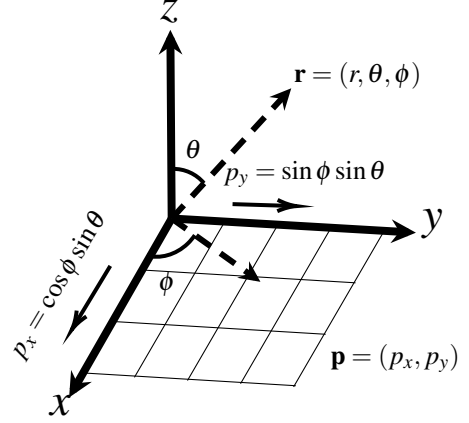


Figure 2. Reference system for the RIS scattered field in the far field. (r, θ, ϕ) and $\mathbf{p} = (p_x, p_y)$ represent the spherical coordinates and the momentum coordinates for the RIS scattered field, respectively.

3 Phase Space Representation

The aim of this work is to predict electromagnetic radiation from RIS surfaces using phase-space simulation methods. In this setting, the EM RIS response and EM re-radiation fields are described statistically, in the form of field-field correlation functions. Here, we work with a correlation function in momentum representation, defined by

$$\Gamma_r(\mathbf{p}', \mathbf{p}'') = \langle \mathbf{E} \cdot \mathbf{E}^* \rangle, \quad (6)$$

where $\mathbf{E}(\mathbf{p}; r)$ is given in Eq.(4), and \mathbf{p}' and \mathbf{p}'' represent the momentum coordinates for the RIS scattered field. The correlation (6) can be used to obtain a phase-space representation of the EM re-radiation from the RIS via the WF. Using this procedure, we find the EM field radiated from the RIS in phase-space, viz.,

$$W_r(\mathbf{x}, \mathbf{p}) = \left[\frac{k}{2\pi} \right]^2 \int d\mathbf{q} e^{j\mathbf{kx} \cdot \mathbf{q}} \Gamma_r \left(\mathbf{p} + \frac{\mathbf{q}}{2}, \mathbf{p} - \frac{\mathbf{q}}{2} \right), \quad (7)$$

where $\mathbf{p} = (\mathbf{p}' + \mathbf{p}'')/2$, $\mathbf{q} = \mathbf{p}' - \mathbf{p}''$ and \mathbf{x} denotes the coordinates of the traced radiation in reference to metasurface coordinates, which is also the inverse Fourier variable of \mathbf{q} . Then the classical RIS reflected phase-space (ray) density is obtained by suitable averaging

$$\rho(\mathbf{x}, \mathbf{p}) \approx \langle W_r(\mathbf{x}, \mathbf{p}) \rangle, \quad (8)$$

where $\langle \cdot \rangle$ represents an appropriate frequency averaging, local (spatial) averaging, or both; this average would be required for a stochastic incident field, but in the current study we are addressing the incidence of a random plane wave. Then $\rho(\mathbf{x}, \mathbf{p})$ can be determined using a fast phase-space propagation method, e.g., DEA, to predict the ray density distribution across large scale environments.

The preliminary results presented in this paper are for a 1D RIS. Figure 3 illustrates a 1D WF obtained for the metasurface unit cell upon normal incidence, at a distance $r = 6\lambda$

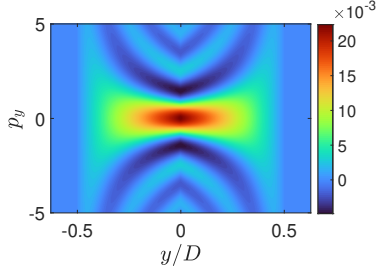


Figure 3. WF obtained for a 1x1 metasurface structure with a normal incidence at distance at distance $r = 6\lambda$.

and with a driven wavenumber $k = 10 [m^{-1}]$. The WF was calculated for an irregular 1x16 metasurface structure under normal plane wave incidence at distance $r = 6\lambda$, as shown in Fig. 4. The red color in the reflection phase mask represents the local phase "1", and the purple color represents the local phase "0". As can be seen, the maximum WF power of the metasurfaces is distributed randomly in all the (propagation) directions. Therefore, there emerges the need to use an optimization tool to focus the maximum WF power in a prescribed direction. In the next section, we show how

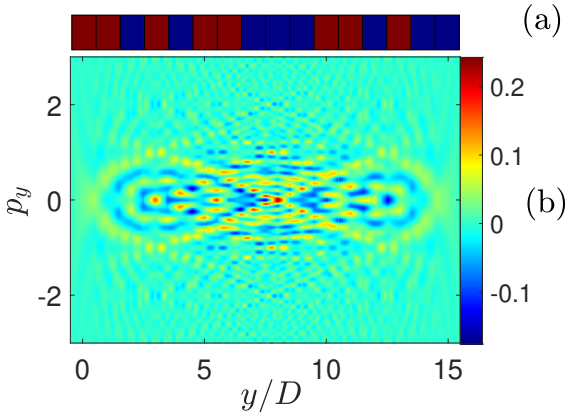


Figure 4. (a) Reflection phase mask for an irregular 1x16 metasurface structure (b) WF obtained for a 1x16 metasurface structure with a random reflection phase mask and a normal incidence at distance at distance $r = 6\lambda$.

to use a simulation-based optimization method to find the ideal reflection state of the RIS for both a beam-splitter and an anomalous reflector.

4 Optimization of Local Reflection Phases

The reflection phase of each pixel is $R_r(n, n)$ as defined in (3) and it can assume values of +1 (state "0") or -1 (state "1") in a binary RIS. An $N \times M$ coding matrix can therefore be used to represent the entire surface. Our goal is to find the optimal reflection phase mask for maximal WF power in a specific wireless propagation direction (upon normal incidence). We use a Simulated Annealing algorithm to find the best reflection phase mask because it has a simple description and has reasonable efficiency. Simulated Annealing is

a method for local searching of minima in functions with complex landscapes. It starts with an initial solution that is updated iteratively with random increments. The initial temperature T , the decreasing rate in each iteration β , the final temperature T_f , the number of iterations I , and the merit function, are the main parameters of Simulated Annealing. In our model, we define an initial reflection phase mask matrix with an equal amount of "0" and "1" that is dispersed randomly. Then the algorithm is evolved by swapping the locations of an arbitrary pair of "0" and "1" to avoid degenerate states. In general, the larger the array, the better the radiated power obtained in the direction of interest. Using this optimization method, the reflection phase mask of the RISs is dynamically tuned to control the EM propagation and obtain the desired far-field wavefront, as shown in Figs. 5 and 6.

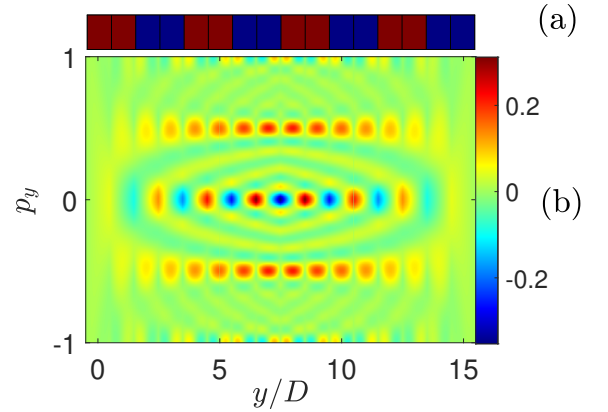


Figure 5. (a) Reflection phase mask for the optimized 1x16 metasurface structure (b) WF obtained for a 1x16 metasurface structure with a random reflection phase mask and a normal incidence at distance at distance $r = 6\lambda$ with desired wireless propagation direction $p_y = \pm \sin(\pi/6)$.

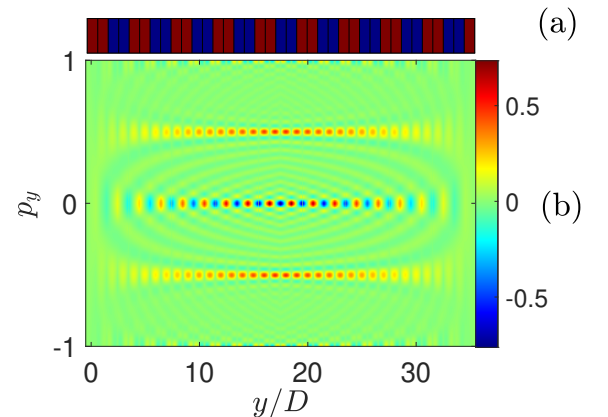


Figure 6. (a) Reflection phase mask for the optimized 1x36 metasurface structure (b) WF obtained for a 1x36 metasurface structure with a random reflection phase mask and a normal incidence at distance at distance $r = 6\lambda$ with desired wireless propagation direction $p_y = \pm \sin(\pi/6)$.

5 Conclusion

In this paper, we present a physics-based modelling approach for evaluating the spatial-angular radiation from an array of reconfigurable unit cells. The model is based on electric/magnetic surface current densities of finite-size, which pixelate the reflecting surface, and allows for the integration of scattered waves from RISs with well-established Eulerian ray-based codes. This extends ray based prediction capabilities by including, besides specular reflection, diffraction, and higher-order EM effects, also the anomalous reflection behaviour achieved by reconfigurable intelligent surfaces. The corresponding phase-space representation is created using a Wigner transform approach for analysing and optimising the design of anomalous reflectors. The results obtained are the first step toward developing a flexible and efficient coverage planning tool for multi-RIS mobile networks. Further work will focus on 2D WF, followed by the implementation of this model within the ray tracing tool DEA to test performance assessments in realistic multi-path propagation scenarios, as well as the development of a ray-based representation of EM radiation from the most important types of reconfigurable engineered surfaces.

6 Acknowledgements

This work has been supported by the European Commission through the H2020 RISE-6G Project under Grant 101017011. The work of Gabriele Gradoni was supported by the Royal Society under Grant INF\R2\192066. In addition to RISE, this work has been partially supported by the EPSRC under Grant EP\V048937\1.

References

- [1] Degli Esposti, V., Vitucci, E.M., Di Renzo, M. and Tretyakov, S., Reradiation and scattering from a reconfigurable intelligent surface: A general macroscopic model, *arXiv e-prints* (2021), pp. arXiv:2107.12107
- [2] M. Di Renzo et al., Smart radio environments empowered by reconfigurable AI meta-surfaces: An idea whose time has come *EURASIP J. Wireless Commun. Netw.* **2019** (2019)
- [3] Q. Wu and R. Zhang, Towards smart and reconfigurable environment: Intelligent reflecting surface aided wireless network, *IEEE Commun. Mag.* **58** (2020), pp. 106–112
- [4] G. Gradoni and M. Di Renzo, End-to-end mutual coupling aware communication model for reconfigurable intelligent surfaces: An electromagnetic-compliant approach based on mutual impedances, *IEEE Wireless Commun. Lett.* **10** (2021), pp. 938–942
- [5] Sihlbom, B., Poulakis, M.I. and Di Renzo, M., Reconfigurable Intelligent Surfaces: Performance Assessment Through a System-Level Simulator, *arXiv e-prints* (2021), pp. arXiv:2111.10791.
- [6] Strinati, E.C., Alexandropoulos, G.C., Sciancalepore, V., Di Renzo, M., Wymeersch, H., Phan-huy, D.T., Crozzoli, M., D’Errico, R., De Carvalho, E., Popovski, P. and Di Lorenzo, P., Wireless environment as a service enabled by reconfigurable intelligent surfaces: The RISE-6G perspective, *arXiv e-prints* (2021), pp. arXiv:2104.06265.
- [7] Rains, J., Tukmanov, A., Cui, T.J., Zhang, L., Abasi, Q.H. and Imran, M.A., High-Resolution Programmable Scattering for Wireless Coverage Enhancement: An Indoor Field Trial Campaign, *arXiv e-prints* (2021), pp. arXiv:2112.11194.
- [8] Ross, C., Gradoni, G., Lim, Q.J. and Peng, Z., Engineering Reflective Metasurfaces with Ising Hamiltonian and Quantum Annealing, (2021),
- [9] Tanner, G., Dynamical energy analysis—Determining wave energy distributions in vibro-acoustical structures in the high-frequency regime, *Journal of Sound and Vibration* **320** (2009), pp. 1023–1038
- [10] Hillery, M. and O’Connell, R.F., Scully, M.O. and Wigner, E.P., Distribution functions in physics: fundamentals, *Physics reports* **106** (1984), pp. 121–167
- [11] Gradoni, G., Creagh, S.C. and Tanner, G. and Smartt, C. and Thomas, D.W.P., A phase-space approach for propagating field–field correlation functions, *New Journal of Physics* **17** (2015), pp. 093027
- [12] G. Gradoni et al., Wigner-Function-Based Propagation of Stochastic Field Emissions From Planar Electromagnetic Sources, *IEEE Transactions on Electromagnetic Compatibility* **60** (2018) pp. 580–588
- [13] Alonso, M. A., Wigner functions in optics: describing beams as ray bundles and pulses as particle ensembles, *Advances in Optics and Photonics* **3** (2011), pp. 272–365
- [14] Mohammed, N. M. and Creagh, S. C. and Tanner, G., Sound radiation from complex vibrating mechanical structures using Wigner transformation techniques *14th Proc. Int. Conf. on Mathematical and Numerical Aspects of Wave Propagation WAVES* (2019), pp. 30
- [15] Mohammed, N. M., Vibroacoustics of complex structures - a wave chaos approach *The University of Nottingham* (2021)
- [16] Kirkpatrick, S., Gelatt, C. D. and Vecchi, M. P., Optimization by Simulated Annealing *Science* **220** (1983), pp. 671–680